3D Super-resolution Using Generalised Sampling Expansion

Hassan Shekarforoush, Marc Berthod, Josiane Zerubia

INSTITUT NATIONAL DE RECHERCHE EN INFORMATIQUE ET EN AUTOMATIQUE

3D Super-resolution Using Generalised Sampling expansion

Hassan Shekarforoush, Marc Berthod, Josiane Zerubia

N° 2706

Novembre 1995

PROGRAMME 4

ISSN 0249-6399

INRIA
SOPHIA ANTIPOLIS

3D Super-resolution Using Generalised Sampling expansion

Hassan Shekarforoush*, Marc Berthod**, Josiane Zerubia***

Programme 4 — Robotique, image et vision
Projet PASTIS

Rapport de recherche n° 2706 — Novembre 1995 — 19 pages

Abstract: Using a probabilistic interpretation of Papoulis' generalized sampling theorem, an iterative algorithm has been devised for 3D reconstruction of a Lambertian surface at sub-pixel accuracy. The problem has been formulated as an optimization one in a Bayesian framework. The latter allows for introducing *a priori* information on the solution, using Markov Random Fields (MRF). The estimated 3D features of the surface are the albedo and the height which are obtained simultaneously using a set of low resolution images.

Key-words: 3D Super resolution, generalized sampling expansion, Low level image processing, Markov Random Fields (MRF).

(Résumé : tsvp)

*hshekar@sophia.inria.fr
**berthod@sophia.inria.fr
***zerubia@sophia.inria.fr

Unité de recherche INRIA Sophia-Antipolis
2004 route des Lucioles, BP 93, 06902 SOPHIA-ANTIPOLIS Cedex (France)
Téléphone : (33) 93 65 77 77 – Télécopie : (33) 93 65 77 65

Super-résolution 3D Par Echantillonnage Multi-canal

Résumé : Dans ce rapport, nous présentons une interprétation probabiliste du théorème d'échantillonnage multi-canal de Papoulis, qui nous permet de mettre en œuvre un algorithme itératif pour la reconstruction 3D d'une surface lambertienne à haute résolution. Le problème est donc formalisé comme celui de la minimisation d'une fonction de coût et il est traité dans un cadre bayesien, ce qui nous permet, d'autre part, d'introduire de l'information *a priori* en utilisant les champs de Markov. Les caractéristiques reconstruites à haute résolution sont l'albedo et l'altitude de la surface observée, qui sont obtenus simultanément à partir d'une séquence d'images à basse résolution.

Mots-clé : Super résolution 3D, échantillonnage multi-canal, traitement d'images bas niveau, champs de Markov.

Table of Contents

1 Introduction

Most super-resolution algorithms proposed in the literature are confined to 2D applications and are concerned with the direct problem of merging low resolution 2D data on a finer grid [9][11][12]. Different methods employed in this group of algorithms, include both frequency domain and spatial domain approaches, extracting sub-pixel information contained in jittered low resolution frames.

In [5][20] a 3D version was proposed where the high resolution albedo of a Lambertian surface was estimated with the knowledge of high resolution height and vice versa. In this paper, the idea has been extended to the inverse problem of simultaneous reconstruction of albedo and height.

The algorithm has been rigorously derived by applying the principle of superposition of linear systems to the extension of Papoulis's generalized sampling Theorem [15] in nD cases and by interpreting it in probabilistic terms.

The problem has, therefore, been formulated as an optimization one in a probabilistic framework with Markov Random fields (MRF) [2] employed for modeling our *a priori* information on the observed data. A generalized simplex algorithm [18] has been proposed for optimizing a cost function iteratively, which in turn yields sub-pixel photometric and geometric information extracted from the low resolution data, given the *a priori* information.

Low resolution image frames have to entail sub-pixel overlap and have to be registered at sub-pixel accuracy. This will imply a preprocessing registration, using methods such as those proposed by [23][22][3][13][19].

Tests have been carried out on both synthetic and real images. The algorithm can be applied in the area of aerial and satellite image processing.

2 Preliminary Assumptions

We shall, henceforth, assume that our sensor is a pin-hole camera located far enough from the observed surface so that the projection of any surface point on the retina of the camera can be regarded as being orthographic. Moreover, camera parameters will be assumed to be known. As for the surface, we shall, hereafter, sample it into a two dimensional array and represent the surface albedo by $g(x,y)$ and the 3D graph of the surface by $z(x,y)$.

Image irradiance will be defined by the impulse response or the Point Spread Function (PSF) $h_w(x,y)$ of the imaging system. The remotely sensed view is usually affected by several impulse response functions: atmosphere h_a, the optics h_o and the sampling aperture h_s. Therefore the resultant PSF is given by $h_a * h_o * h_s$ (where $*$ denotes convolution). Each component introduces a type of smoothing operation and as a result, the net effect of these components in a complex remote sensing system can often be quite reasonably approximated by a 2D Gaussian pulse with a radius of gyration which depends on the resolution constraints of the imaging system [21]. In general the PSF can be approximated by:

$$h_{w_{xy}}(x_1,y_1) = Kexp\left(\frac{1}{2(1-\alpha^2)}\left(\frac{x_1^2}{w_{x1}^2} - \frac{2\alpha}{w_{x1}w_{y1}}x_1y_1 + \frac{y_1^2}{w_{y1}^2}\right)\right) \tag{1}$$

where K is a constant depending on the gain of the system, w_{x1} and w_{y1} are the radii of gyration about the two axes and α is the coupling factor between two directions. Using the following rotational transformation of our reference frame [21]:

$$\begin{cases} x = x_1cos\varphi - y_1sin\varphi \\ y = x_1sin\varphi + y_1cos\varphi \\ \varphi = \frac{1}{2}tan^{-1}\left(\frac{2\alpha w_{x1}w_{y1}}{w_{x1}^2 - w_{y1}^2}\right) \\ w_x^2 = w_{x1}^2cos^2\varphi - w_{y1}^2sin^2\varphi \\ w_y^2 = w_{x1}^2sin^2\varphi + w_{y1}^2cos^2\varphi \end{cases} \tag{2}$$

we will obtain:

$$h_{w_{xy}}(x,y) = Kexp\left(-\frac{1}{2}\left(\frac{x^2}{w_x^2} + \frac{y^2}{w_y^2}\right)\right) \tag{3}$$

For the case where the gray levels are preserved by the system [21], we have $K = \frac{1}{2\pi w_x w_y}$. Therefore assuming a circulary-symmetric (isotropic) Gaussian function the radius of gyration about both axes will be equal and given by $w = \sigma$, where σ is the standard deviation of the kernel. Thus:

$$h_w(x,y) = \frac{1}{2\pi\sigma^2} exp(-\frac{x^2+y^2}{2\sigma^2}) \tag{4}$$

Therefore, by including a PSF [1][17] in our image formation model, we distinguish our image irradiance equation from the one defined in shape from shading algorithms [10]. Thus, assuming shift invariance the image irradiance is given by:

$$I(k,l) = \sum_{(x,y)\in w} h_w(x-x_c, y-y_c)\; g(x,y)R(x,y) \tag{5}$$

where $I(k,l)$ is the image intensity at coordinates (k,l), $h_w(x-x_c, y-y_c)$ is the PSF shifted by (x_c, y_c), and $R(x,y)$ is the reflectance function of the Lambertian surface, whose product with the albedo $g(x,y)$ yields the luminance energy at coordinates (x,y) in the sampled array. The reflectance function is, in fact, a function of the normal to the surface (see [4] for details).

Camera coordinates (k,l) are related to the world coordinate frame by:

$$k = a_{11}x + a_{12}y + a_{13}z + a_{14} \tag{6}$$

$$l = a_{21}x + a_{22}y + a_{23}z + a_{24} \tag{7}$$

Assuming that camera motions from one low resolution frame to another are only composed of translation and rotation around the origin of the world frame [8]:

$$a_{11} = a_{22} = S_x cos\theta \tag{8}$$

$$-a_{12} = a_{21} = S_y sin\theta \tag{9}$$

where S_x and S_y are the ratios of the sampling rates of the desired high resolution images to those of the low resolution frames along x and y axes, respectively, and θ is the rotation angle of the camera around the origin of the world frame. Working on square images of widths d and D for the low resolution and the high resolution frames, respectively, and assuming uniform and equal sampling rates along

both axes, we have: $S_x = S_y = \frac{d}{D}$. As for other camera parameters, we have set $a_{13} = a_{23} = 0$ and a_{14} and a_{24} depend on the translation of the camera along the two axes. The latter should be in such a way that sub-pixel overlap is obtained between pixels of any two observed images in the sequence.

3 Problem Statement and Proposed Solution

We can, now, formulate the problem as that of solving equation (5) for g and z, which is a special case of the image irradiance equation [10][4]. To this end we need to recall some definitions as well as the generalized sampling theorem in n dimensions:

Unless otherwise mentioned, all functions are n-dimensional vector functions and $f(\vec{t}) \leftrightarrow \mathcal{F}(\vec{\omega})$ denote a Fourier transform pair.

Definition: *A finite energy function $f(\vec{t})$ [16] is said to be σ-band limited if its Fourier transform $\mathcal{F}(\vec{\omega}) = 0$ outside the finite size hypercube $\mid \omega_i \mid \geq \sigma_i$, $i = 1 \ldots n$.*

Theorem: *nD Generalised Sampling Theorem*
We apply a σ-band limited function $f(\vec{t})$ as a common input to m independent linear shift invariant systems with transfer functions $\mathcal{H}_1(\vec{\omega}) \ldots \mathcal{H}_m(\vec{\omega})$. The resulting outputs are:

$$\phi_r(\vec{t}) = \frac{1}{(2\pi)^n} \int_{-\sigma_1}^{\sigma_1} \ldots \int_{-\sigma_n}^{\sigma_n} \mathcal{F}(\vec{\omega}) \mathcal{H}_r(\vec{\omega}) exp(j\vec{\omega}^T \vec{t}) d\omega_1 \ldots d\omega_n \tag{10}$$

where $r = 1 \ldots m$, $\omega_1 \ldots \omega_n$ are the components of $\vec{\omega}$ and T denotes the transposition. Next, we sample these outputs at $\frac{1}{m}$th of the Nyquist rate along each dimension, ie. with a sampling matrix S whose diagonal terms are $\frac{m\pi}{\sigma_i}$:

$$S = [s_{ab}] \ , \ s_{ab} = \frac{m\pi}{\sigma_i} \ if \ a = b = i \tag{11}$$

It can be shown that [7] :

$$f(\vec{t}) = \sum_{r=1}^{m} \sum_{k_1=-\infty}^{\infty} \ldots \sum_{k_n=-\infty}^{\infty} \phi_r(S\vec{k}) y_r(\vec{t} - S\vec{k}) \tag{12}$$

where $\vec{k} = [k_1 \ldots k_n]$ is an integer valued vector and:

$$y_r(\vec{t}) = \frac{\mid S \mid}{(2\pi)^n} \int_{-\sigma_1}^{\sigma_1 + c_1} \ldots \int_{-\sigma_n}^{\sigma_n + c_n} Y_r(\vec{\omega}, \vec{t}) exp(j\vec{\omega}^T \vec{t}) d\omega_1 \ldots d\omega_n \tag{13}$$

$Y_r(\vec{\omega},\vec{t})$ are given by the following set of simultaneous equations:

$$\sum_{r=1}^{m}\mathcal{H}_r(\vec{\omega}+(\ell-1)\vec{c})Y_r(\vec{\omega},\vec{t})=exp(j(\ell-1)\vec{c}^T\vec{t})\ ,\ \ell=1\ldots m \tag{14}$$

where $\vec{c}=[\frac{2\sigma_1}{m}\ldots\frac{2\sigma_n}{m}]$ *and* $-\sigma_i\leq\omega_i\leq-\sigma_i+\frac{2\sigma_i}{m}$.

The system of equations (14) has got a solution since $\mathcal{H}_r$ are assumed to be independent. Therefore, we will find cyclic values (see [16]) for $Y_r(\vec{\omega},\vec{t})$. Moreover, let us make the same assumption as Papoulis that $Y_r(\vec{\omega},\vec{t})$ admit Fourier series expansion in the finite size hypercube $\mid\vec{\omega}_i\mid\geq\sigma_i>0\ ,\ i=1\ldots n$. It is then obvious that $y_r(\vec{t})$ (which may be considered as the impulse responses of optimal post-filtering operations) will vanish iff the sampling matrix is singular, ie the n-dimensional expansion in (12) is valid iff the sampling matrix S is non-singular.

Since digital images are, usually, sampled on a rectangular grid, we will, hereafter, assume that S is diagonal. This implies that the samples along each dimension are taken independently. Note also that since $\sigma_i>0$ are finite, S will always be non-singular in this case.

Now, let the number of available low resolution frames be $\ell<m$ then by simply applying the principle of superposition, one can attempt to reconstruct a sample of $f(\vec{t})$ at the resolution $\frac{\ell}{m}$th of the Nyquist rate along each dimension:

$$\begin{aligned}f(\vec{t})=&\sum_{r=1}^{\ell}\sum_{k_1=-\infty}^{\infty}\ldots\sum_{k_n=-\infty}^{\infty}\phi_r(S\vec{k})y_r(\vec{t}-S\vec{k})\\&+\sum_{r=\ell+1}^{m}\sum_{k_1=-\infty}^{\infty}\ldots\sum_{k_n=-\infty}^{\infty}\phi_r(S\vec{k})y_r(\vec{t}-S\vec{k})\end{aligned}\tag{15}$$

Therefore:

$$f_\ell(\vec{t})=\sum_{r=1}^{\ell}\sum_{k_1=-\infty}^{\infty}\ldots\sum_{k_n=-\infty}^{\infty}\phi_r(S\vec{k})y_r(\vec{t}-S\vec{k})\tag{16}$$

where $f_\ell(\vec{t})$ is a sample of $f(\vec{t})$ at $\frac{\ell}{m}$th of the Nyquist rate along each dimension.

In probabilistic terms equation (16) is equivalent to minimizing the convergence error in the mean square sense:

$$\epsilon^2 = \mathcal{E}\{(f_\ell(\vec{t}) - \sum_{r=1}^{\ell} \sum_{k_1=-\infty}^{\infty} \dots \sum_{k_n=-\infty}^{\infty} \phi_r(S\vec{k}) y_r(\vec{t} - S\vec{k}))^2\} \tag{17}$$

where $\mathcal{E}$ represents the expected value.

Alternatively, we can minimize the error after sampling. Threfore, if $\hat{\phi}_r(S\vec{k})$ denotes an estimate of $\phi_r(S\vec{k})$, then:

$$\epsilon_\phi^2 = \mathcal{E}\{\sum_{r=1}^{\ell} (\phi_r(S\vec{k}) - \hat{\phi}_r(S\vec{k}))^2\} \tag{18}$$

An interesting situation arises when $f_\ell(\vec{t})$ is expressed in terms of two (or more) variables (eg. albedo and height): $f_\ell(\vec{t}) = f_\ell(\vec{s}_1(\vec{t}), s_2(\vec{t}))$. We can then seek high resolution information for $s_1(\vec{t})$ and $s_2(\vec{t})$. This is obviously an inverse problem and can be tackled using regularization or equivalently MRF's.

The n-dimensional extension of Papoulis' sampling expansion is an ideal tool for our purpose. In this context, in a sequence of low resolution images, each frame can be assumed to contain the recuring samples of a nonuniform sampling sequence obtained by applying a common input function to a set of linear shift invariant systems. We, obviously, need to register the recuring samples using registration algorithms such as [23][22][3][13][19].

Let g and z denote the vectors of unknown variables, ie. the vectors of the albedo $g_{(x,y)}$ and the height $z_{(x,y)}$ on the super-resolution grid at $\frac{\ell}{m}$th of the Nyquist rate. Here, the input is a function of g and z: $f(g,z)$ (see Appendix A). Let also I denote the vector of all observed pixel values in our low resolution frames. Then using Bayes law on probability distributions and assuming that g and z are independent:

$$p(g,z \mid I) = K\ p(I \mid g,z)\ p(g)p(z) \quad , \quad \text{where } K \text{ is a constant} \tag{19}$$

Applying the Hammersley-Clifford theorem [14] to $p(g)$ and $p(z)$ and assuming a Gaussian distribution for $p(I \mid g,z)$ we can calculate the Maximum a Posteriori

(MAP) estimator as follows:

$$E(g,z) = -ln\ p((g,z) \mid I) = e^T C_e^{-1} e + u_g^T C_g^{-1} u_g + u_z^T C_z^{-1} u_z + constant \qquad (20)$$

Using a membrane model for $p(g)$ and $p(z)$ [6], and assuming that $e^T C_e^{-1} e = \epsilon_\phi^2$, given by (18), we can write the following cost function at any point (x,y) of our sampled array:

$$E_{(x,y)} = \sum_{\ell} \sum_{(k',l') \in \nu_{(\mathrm{k,l})}} \frac{(I^{\ell}_{(k',l')} - \hat{I}^{\ell}_{(k',l')})^2}{2\sigma_e^2} + \sum_{(x',y') \in \nu_{(\mathrm{x,y})}} \frac{(\hat{g}_{(x,y)} - \hat{g}_{(x',y')})^2}{2\sigma_g^2} + \sum_{(x',y') \in \nu_{(\mathrm{x,y})}} \frac{(\hat{z}_{(x,y)} - \hat{z}_{(x',y')})^2}{2\sigma_z^2} \qquad (21)$$

where $\nu_{(\mathrm{k,l})}$ is the set of all pixels in the neighbourhood of (k,l) whose intensities are affected by the irradiance at (x,y) (depending on the support of h, see Appendix A), $\nu_{(\mathrm{x,y})}$ is the neighbourhood structure depending on the order of the MRF associated with the estimates $\hat{g}$ and $\hat{z}$, σ_e^2, σ_g^2 and σ_z^2 are the variances of the error vector, g and z, respectively. Therefore, the MAP estimator amounts to minimizing (21) for which we have employed a generalized simplex algorithm [18]. Equation (21) has been obtained by approximating the covariance matrices as being diagonal with constant terms on the diagonal.

4 An Algorithmic view

The algorithm is iterative and is shown schematically in Figure 1. We proceed as follows: first, we initialize it using a set of low resolution images. The imaging process is then simulated to create a set of low resolution estimates of sensor observations. The objective function in (21) characterizing the estimation error and the Gibbs energy of our MRF is minimized simultaneously with respect to the albedo and the surface height. The algorithm is repeated iteratively until no more reduction in the objective function is achieved for a preset number of successive iterations.

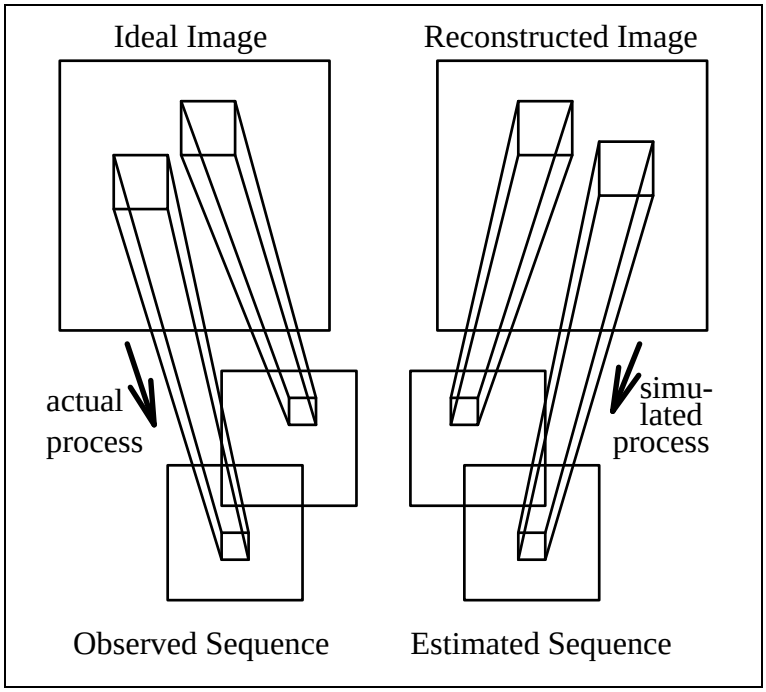

Figure 1: Schematic diagram of the algorithm

The major obstacle is the non-convexity of the objective function. Different optimization algorithms have been proposed in the literature for minimising a non-convex function which have been briefly compared in [4]. In this article, we have considered the use of a generalized simplex algorithm which is based on the idea of constructing a non-local linear approximation of a function by updating an n-dimensional simplex in $\mathbb{R}^n$ (see [18] for details). We have initialized the simplex algorithm using a set of low resolution images and a noisy/sparse low resolution height map.

5 Experimental Results

In this section we present some tests on both synthetic and real data. Signal to Noise Ratio (SNR) is used for measuring the quality of results. Original images were 50×50 and 100×100 for low resolution and high resolution, respectively.

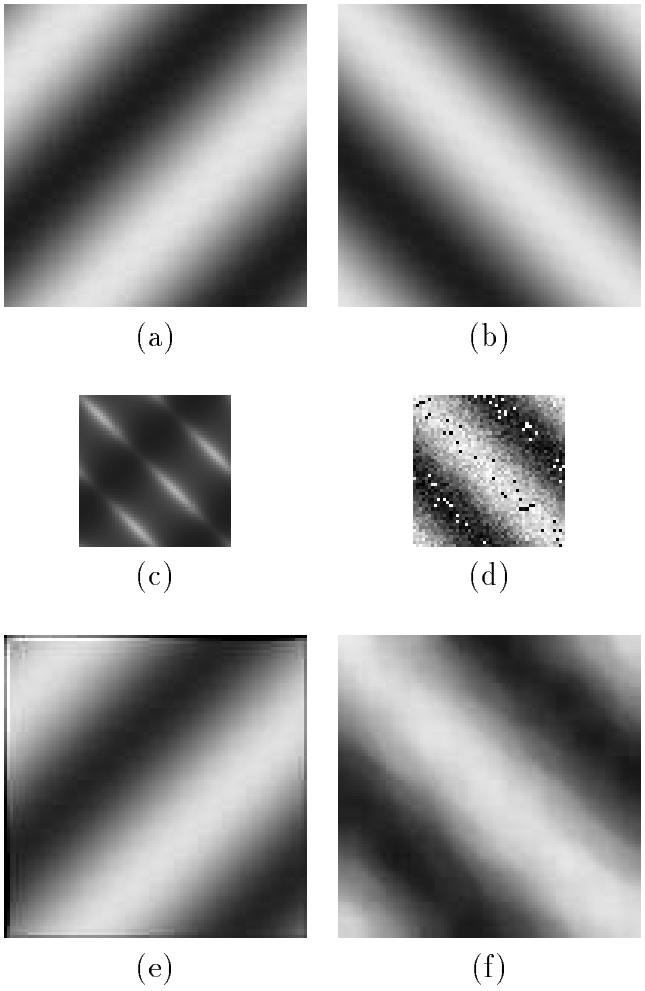

Figure 2: (a), (b) albedo & height, (c) one of the simulated low resolution camera images, (d) a noise corrupted low resolution height SNR=5 dB, (e) reconstructed albedo SNR=34 dB, (f) reconstructed height SNR=27 dB

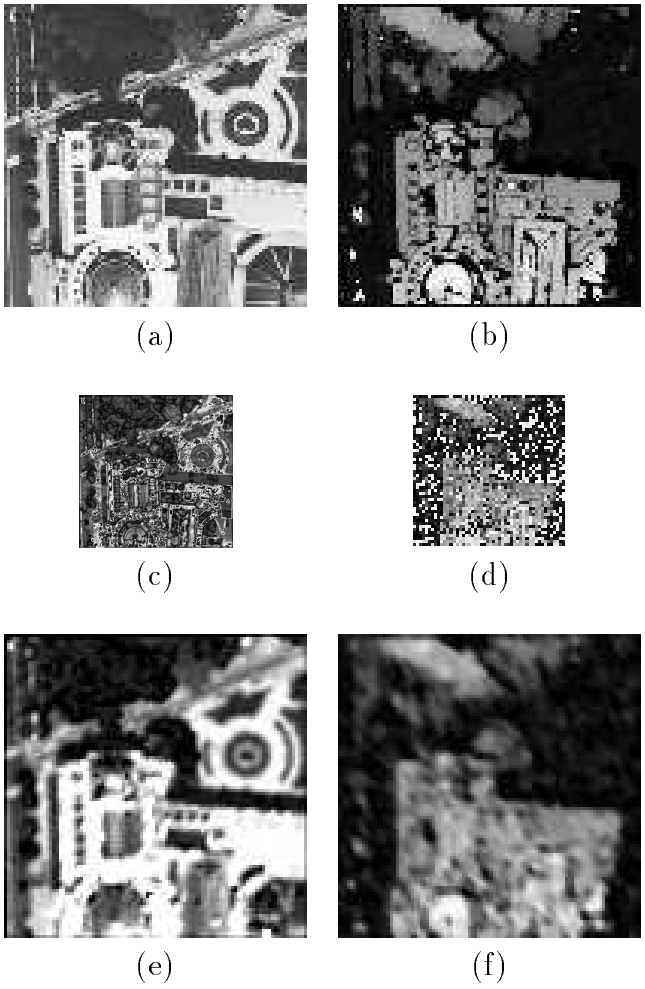

Figure 3: (a) albedo, (b) height, (c) one of the low resolution camera images, (d) a noise corrupted low resolution height SNR=5 db, (e) reconstructed albedo SNR=25 dB, (f) reconstructed height SNR=22 dB

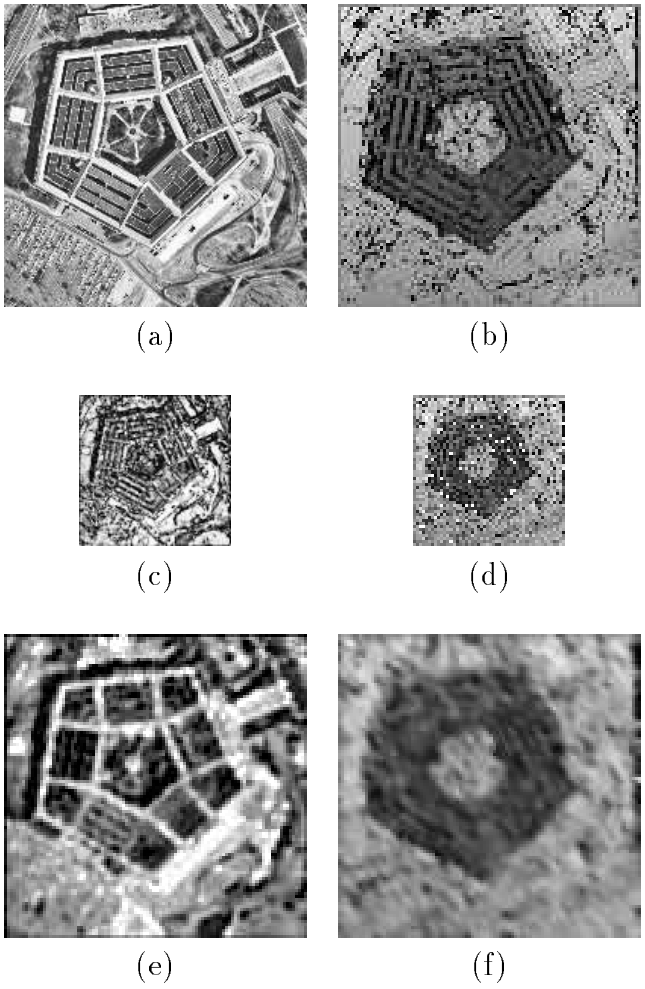

Figure 4: (a) albedo, (b) height, (c) one of the simulated low resolution camera images, (d) a noise corrupted low resolution height SNR=5 db, (e) reconstructed albedo SNR=26 dB, (f) reconstructed height SNR=24 dB

6 Conclusion

Using a probabilistic interpretation of Papoulis' generalized sampling theorem, it is possible to reconstruct, simultaneously, sub-pixel information on the albedo and the height of a Lambertian surface, provided that a sequence of independent images have been given at a lower resolution, and that they have been registered at subpixel accuracy. The problem has been shown to reduce to that of data fusion in 3D. The Lambertian assumption is not restrictive, since the formulation would allow adopting other imaging models, if required.

Two main problems were encountered when testing the algorithm: one is the trade-off between the regularization term and the error term in the cost function, which proved to be not so easy when dealing with real images. For the synthetic image the problem was almost non-existent due to the fact that the test images did not exhibit discontinuities. This problem could, therefore, be handled by taking into acount a discontinuity field and hence by including extra terms in the cost function. The second problem was the convergence of the simplex algorithm which, apparently, slows down as we get closer to the optimum point. A possible solution would be to switch to a gradient method in the neighbourhood of the solution where the cost function exhibits convexity. The simplex algorithm, however, is robust to noise and is very efficient far from the solution.

Since the problem has been formulated as a constrained optimization one, further extensions of the proposed method can be considered along the same direction. Therefore, we might consider optimizing with respect to parameters of the imaging system which could yield for example the optimal light source direction, etc.

Appendix A

The input to our linear systems is, merely, the Lambertian imaging function defined by:

$$f(g(\vec{t}), z(\vec{t})) = g(\vec{t})R(\vec{t}) \tag{22}$$

where $\vec{t} = (x, y)$, g is the albedo of the surface which is assumed to be varying and R is the reflection function of the surface which depends on the direction of the local normal to the surface. The latter is given by local variations of height, ie. the partial derivatives of $z(\vec{t})$ along each dimension (see [5][10] for details). In our case, for example, the local normal will be given by $(\frac{\partial z}{x}, \frac{\partial z}{y}, -1)$.

We have assumed a Gaussian kernel for the linear shift invariant systems and therefore the imaging model prior to discretization is given by a convolution integral:

$$\phi_r(\vec{t}) = \int_{-\infty}^{\infty}\int_{-\infty}^{\infty} h(\vec{t} - \vec{\tau})g(\vec{t})R(\vec{t})\, dx\, dy \tag{23}$$

where τ is a shift vector. In practice, the support of H is approximated by a finite size window. Fourier transforming the right hand side and using the convolution theorem, we can easily verify that this equation corresponds to equation (1). Note also that $\phi_r(\vec{t})$ are continuous versions of our discrete images given by $I_{(k,l)}$, where camera coordinates (k, l) are related to the world coordinate frame by: $[k, l]^T = A\ [x, y, z, 1]^T$ where A is a 2×4 matrix containing camera parameters. The last column of A contains the interframe shift parameters, specifying the coregistration of image frames. Other parameters specify the sampling rate along the two axes and the rotation of the camera around the origin (for further details see [8][20]).

References

[1] H. C. Andrews and B. R. Hunt. *Digital Image Restoration.* Prentice-Hall Inc., 1st edition, 1977.

[2] R. Azencott. Image analysis and markov fields. In *Int. Conf. Ind. & Appl. Math*, Paris, 1987. SIAM.

[3] C. A. Bernstein, L. N. Kanal, D. Lavin, and E. C. Olson. A geometric approach to subpixel registration accuracy. *CVGIP*, 40:334–360, 1987.

[4] M. Berthod, H. Shekarforoush, M. Werman, and J. Zerubia. Reconstruction of high resolution 3d visual information, 1993. INRIA research report, France.

[5] M. Berthod, H. Shekarforoush, M. Werman, and J. Zerubia. Reconstruction of high resolution 3d visual information. In *Proc. CVPR*, pages 654–657, Seattle, Washington, 1994.

[6] A. Blake and A. Zisserman. *Visual Reconstruction.* MIT Press, 1987.

[7] K. F. Cheung and R. J. Marks. Papoulis' generalization of the sampling theorem in higher dimensions and its applications to sample density reduction. In *Proc. Int. Conf. on circuits and systems*, Nanjing, China, 1989.

[8] E. De Castro and C. Morandi. Registration of translated and rotated images using finite fourier transforms. In *IEEE PAMI*, volume 9, No 5, pages 700–703, 1987.

[9] D. Gross. Super-resolution from sub-pixel shifted pictures. Master's thesis, Tel-Aviv University, Oct. 1986.

[10] B. K. P. Horn. Understanding image intensities. *Artificial Intelligence*, 8(2):201–231, 1977.

[11] M. Irani and S. Peleg. Super-resolution from image sequences. Technical Report 89-7, The Hebrew University of Jerusalem, June 1989.

[12] D. Keren, S. Peleg, and R. Brada. Image sequence enhancement using sub-pixel displacement. In *Proc. CVPR*, pages 742–746, Ann Arbor, June 1988.

[13] S. P. Kim and Wen-Yu Su. Subpixel accuracy image registration by spectrum cancellation. In *Proc. ICASSP*, pages 153–156, San Fransisco, 1993.

[14] J. Moussouris. Gibbs and markov random systems with constraints. *Journal of Statistical Physics*, 10(1), 1974.

[15] A. Papoulis. Generalized sampling expansion. In *IEEE Trans. on Circuits and Systems*, volume 24, No 11, Nov. 1977.

[16] A. Papoulis. *Signal Analysis*. McGraw-Hill Book Company, 1977.

[17] A. Rosenfeld and A. C. Kak. *Digital Picture Processing*, volume 1 and 2. Academic Press Inc., 1982.

[18] H. Shekarforoush, M. Berthod, and J. Zerubia. Direct search generalized simplex algorithm for optimizing non-linear functions. research report N^o 2535, INRIA - France, 1995.

[19] H. Shekarforoush, M. Berthod, and J. Zerubia. Subpixel image registration by estimating the polyphase decomposition of cross power spectrum. research report 2707, INRIA - France, 1995.

[20] H. Shekarforoush, M. Berthod, J. Zerubia, and M. Werman. Sub-pixel bayesian estimation of albedo and height. *International Journal of Computer Vision*, to appear.

[21] D. S. Simonett and F. T. Ulaby, editors. *Manual of Remote Sensing*, volume 1. American Society of Photogrammetry, second edition, 1983.

[22] Qi Tian and M. N. Huhns. Algorithms for subpixel registration. *CVGIP*, 35:220–223, 1986.

[23] R. Tsai and T. Huang. Multiframe image restoration and registration. *Adv. Comp. Vis. Im. Proc.*, 1, 1984.

Unité de recherche INRIA Lorraine, Technopôle de Nancy-Brabois, Campus scientifique,
615 rue du Jardin Botanique, BP 101, 54600 VILLERS LÈS NANCY
Unité de recherche INRIA Rennes, Irisa, Campus universitaire de Beaulieu, 35042 RENNES Cedex
Unité de recherche INRIA Rhône-Alpes, 46 avenue Félix Viallet, 38031 GRENOBLE Cedex 1
Unité de recherche INRIA Rocquencourt, Domaine de Voluceau, Rocquencourt, BP 105, 78153 LE CHESNAY Cedex
Unité de recherche INRIA Sophia-Antipolis, 2004 route des Lucioles, BP 93, 06902 SOPHIA-ANTIPOLIS Cedex

Éditeur
INRIA, Domaine de Voluceau, Rocquencourt, BP 105, 78153 LE CHESNAY Cedex (France)
ISSN 0249-6399